Journal of Advanced Marine Engineering and Technology, Vol. 49, No. 3, pp. 107~115, 2025
J. Advanced Marine Engineering and Technology (JAMET)
https://doi.org/10.5916/jamet.2025.49.3.107

ISSN 2234-7925 (Print)
ISSN 2765-4796 (Online)
Original Paper

Effects of supercharging on combustion and NOx emission characteristics under various relative air-to-fuel ratios in a hydrogen DISI engine

Seungjae Kim[1] · Hyungmin Lee[2] · Kyoungdoug Min[†]

(Received May 19, 2025 ; Revised June 4, 2025 ; Accepted June 18, 2025)

Abstract: The focus of this study is an experimental analysis of the effects of increasing the intake pressure on combustion characteristics and NOx emissions under various relative air-to-fuel ratios with a hydrogen direct injection spark ignition (DISI) single-cylinder engine. The engine speed was set to 1500 rpm, and the relative air-to-fuel ratio was changed by controlling the amount of injected hydrogen. The intake pressure was changed from 0.10 MPa to 0.14 MPa with an interval of 0.2 MPa using a supercharger. The results revealed that increasing the intake pressure from 0.10 MPa to 0.14 MPa decreased the coefficient of variation in the gross mean effective pressure from 5.79% to 1.02% at λ=3.5 because of faster flame development. Owing to higher combustion stability for an intake pressure of 0.14 MPa, the operable relative air-to-fuel ratio toward lean conditions was extended, resulting in 47.13% gross thermal efficiency with 4 ppm NOx emissions at λ=4.0. In addition, the gross mean effective pressure increased with increasing intake pressure under various relative air-to-fuel ratio conditions. Specifically, the maximum gross mean effective pressures were 0.80, 0.95, and 1.02 MPa for intake pressures of 0.10, 0.12, and 0.14 MPa, respectively.

Keywords: Hydrogen DISI engine, Intake pressure, Relative air-to-fuel ratio, Combustion stability, Gross mean effective pressure, NOx emissions

Nomenclature

ABDC	After bottom dead center
ATDC	After top dead center
BBDC	Before bottom dead center
BDC	Bottom dead center
BTDC	Before top dead center
CA	Crank angle
CKPS	Crank position sensor
CMPS	Camshaft position sensor
CO_2	Carbon dioxide
CoV_{GMEP}	Coefficient of variation of the gross mean effective pressure
DISI	Direct injection spark ignition
ECU	Engine control unit
GMEP	Gross mean effective pressure
GTE	Gross thermal efficiency
H_2	Hydrogen
HRR	Heat release rate
ICE	Internal combustion engine
IGN	Ignition
nIMEP	Net indicated mean effective pressure
NOx	Nitrogen oxides
MBT	Maximum brake torque
MFB	Mass fraction burned
MPRR	Maximum pressure rise rate
m_{fuel}	Mass of injected fuel
P	In-cylinder pressure
$P_{compression}$	In-cylinder pressure during the compression stroke
$P_{expansion}$	In-cylinder pressure during the expansion stroke
Q_{LHV}	Lower heating value
rpm	Rotation per minute

† Corresponding Author (ORCID: http://orcid.org/0000-0002-1201-6312): Professor, Department of Mechanical Engineering, Seoul National University, 1 Gwanak-ro, Gwanak-gu, Seoul 08826, Korea, E-mail: kdmin@snu.ac.kr, Tel: 02-880-1661

1 Instructor, Department of Navigation and Ship Handling System, Republic of Korea Naval Academy, E-mail: seungjaekim@navy.ac.kr, Tel: 055-907-5346

2 Professor, Department of Navigation and Ship Handling System, Republic of Korea Naval Academy, E-mail: hmsj1226@naver.com, Tel: 055-907-5230

V	In-cylinder volume
V_{TDC}	In-cylinder volume at the top dead center
V_{BDC}	In-cylinder volume at the bottom dead center
V_d	Displaced volume
γ	Specific heat ratio
θ	Crank angle
λ	Relative air-to-fuel ratio
σ_{GMEP}	Standard deviation in gross mean effective pressure

1. Introduction

Climate change resulting from global warming requires urgent, global-level solutions to reduce carbon dioxide (CO_2) emissions in all industrial sectors. In particular, the maritime sector, which accounts for 11.2% of CO_2 emissions from the transportation industry and emitted approximately 0.89 Gt of CO_2 in 2022, represents a major concern in efforts to reduce CO_2 emissions across all industrial sectors **[1]**.

To reduce CO_2 emissions in the maritime sector, the adoption of hydrogen-based fuels—a type of low-carbon fuel—has been proposed as a promising solution **[2]**. In particular, hydrogen (H_2) is gaining attention as a next-generation internal combustion engine (ICE) fuel to replace fossil fuels, as it is a carbon-free fuel that is emitted without CO_2 from combustion and possesses properties suitable for ICE applications **[3][4]**.

However, the high combustion temperature of hydrogen results in significant nitrogen oxide (NOx) emissions **[5]**, which are considered a major drawback of H_2-ICEs. Accordingly, ongoing research efforts are being made to address this issue.

One of the effective methods to reduce NOx emissions in H_2-ICEs is lean operation, which results in a lean relative air-to-fuel ratio (λ) to reduce the combustion temperature **[6]**. For example, a study by Wallner et al. **[7]** demonstrated that operating an engine at λ=3.0 resulted in NOx emissions that were 100 times lower than those during operation at λ=2.0 under conditions of 1,500 rpm and an engine torque of 25 Nm. Furthermore, Fu et al. **[8]** demonstrated that increasing λ is more effective in reducing NOx emissions than optimizing the ignition timing. Specifically, under all ignition timing conditions, the NOx emissions at $\lambda = 2.0$ were lower than those at $\lambda = 1.0$ and 1.5.

Although increasing λ effectively decreases the amount of NOx emissions, lean operation has the drawback of a reduced engine load due to the lower fuel concentration in the air/fuel mixture **[4]**. To address this issue, various methods, including optimizing the valve timing or adopting chargers, have been studied **[9]-[11]**. For example, Lee **[9]** increased the maximum net indicated mean effective pressure (nIMEP) of an H_2-ICE under naturally aspirated conditions from 0.574 MPa to 0.712 MPa with an increase in λ from 1.5 to 2.2 by advancing the intake valve timing and exhaust valve timing by 40° CA and 38° CA, respectively. Furthermore, the study of Verhelst et al. **[10]** indicated that adopting a supercharger increased the brake power of an H_2-ICE by 40% compared with atmospheric operation under conditions where NOx emissions were limited to 100 ppm. In addition, Nguyen et al. **[11]** demonstrated that the use of a supercharger in an H_2-ICE resulted in approximately 15% greater net power output than did a turbocharger under low-load conditions at 2000 rpm.

Although various studies have been conducted to increase the output of H_2-ICEs under lean conditions, many researchers **[4][9][12]** have emphasized the need for H_2-specific injectors capable of rapidly injecting gaseous H_2 fuel. The fundamental issue is that conventional injectors, which were originally designed for liquid fuels, exhibit low injection rates when used with gaseous H_2, making it difficult to supply enough fuel. Moreover, the low injection rates retard the end of fuel injection timing, leading to the formation of a stratified mixture and a consequent increase in NOx emissions, which poses a significant challenge **[13]**.

To mitigate these challenges, several studies have explored the advancement of fuel injection timing using conventional injectors. However, a significant issue remains, as the rate of increase in NOx emissions surpasses that of power output enhancement. For example, Lee **[9]** advanced the fuel injection timing from BTDC 120° to BTDC 160° to improve the gross mean effective pressure (GMEP). Although the maximum GMEP increased by 15.4%, the NOx emissions more than doubled.

Recently, studies have demonstrated the successful use of H_2-specific injectors to achieve both high engine output and low NOx emissions. For example, Kim **[14]** reported that with the use of hydrogen injectors, even with a 40-degree delay in fuel injection timing, the maximum GMEP achievable under naturally aspirated conditions was approximately 0.1 MPa higher than that obtained with a conventional gasoline injector, whereas NOx emissions were reduced by more than half. However, the use of H_2-specific injectors under naturally aspirated conditions has been reported to result in lower combustion stability under ultra-lean conditions, where NOx emissions are reduced **[8][14]-[16]**. Furthermore, research exploring the effects of H_2-specific

injectors on the combustion characteristics and NOx emissions of H_2-ICEs under boosted conditions is lacking.

Therefore, this study was conducted to investigate the effects of using an H_2-specific injector in an H_2 direct injection spark ignition (DISI) engine on combustion characteristics and NOx emissions under various boosted conditions. Specifically, the focus of this study is on analyzing combustion characteristics, such as burn duration and combustion stability, under various intake pressures and relative air-to-fuel ratios. Additionally, the effects on engine performance, thermal efficiency, and NOx emissions were also analyzed.

2. Experimental Setup

2.1 Experimental Apparatus

A 0.5 SI single-cylinder research engine with a compression ratio of 12 was used for the experiment. The main specifications of the test engine are shown in **Table 1**.

For the control of the engine, a Motec-m800 engine control unit (ECU) was used. Because the ECU was connected to a computer with the installed control program, the signals from the crankshaft position sensor (CKPS) and the camshaft position sensor (CMPS) were acquired. Additionally, the ECU produced signals to control the duration and timing of ignition and the injection system. To transmit a specific signal to the ECU to determine the cycle interval, a National Instrument cRIO-9039, which received the engine rotation speed from an encoder and produced a real-time pulse signal every two revolutions, was used. A 190 kW AVL ELIN AC dynamometer was used to control the engine speed and throttle valve.

For hydrogen fuel injection, a PHINIA outwardly opened H_2 injector, specifically designed for hydrogen gas injection, was directly mounted on the side of the engine. The fuel injection pressure was set at 3 MPa.

The mass flow rate of the injected fuel was measured using a Coriolis-type real-time fuel mass flowmeter (OVAL CA001). A Horiba MEXA-110 λ sensor was installed at the end of the exhaust manifold to measure the relative air-to-fuel ratio (λ). A flush-mounted piezoelectric pressure sensor (Kistler 6056A) was installed on the cylinder to measure the in-cylinder pressure. The Kistler 4007C was used for measuring absolute pressure of intake pressure, and combustion analysis was performed using a combustion analyzer (Kistler Kibox to go 2893).

The combustion results, including in-cylinder pressure traces, were aligned to the crank angle (CA) domain based on the CKPS signal and recorded in units of 0.1 °CA for 200 cycles. The NOx emissions were measured using an emissions analyzer (Horiba MEXA-7100 DEGR). To increase the intake pressure, a supercharger was installed before the intake manifold. To ensure the accuracy of the experimental data, all sensors and equipment were calibrated before the experiment.

To maintain the temperature of the intake air below 40 °C, a water-cooled intercooler was installed at the front end of the intake manifold. A schematic of the experimental setup is presented in **Figure 1,** and specifications for sensors and equipment are detailed in **Table 2**.

Table 1: Main specifications of the research engine

Item	Descriptions	
Displacement [L]	0.5	
Compression ratio	12	
Stroke [mm]	111	
Bore [mm]	75.6	
Connecting rod [mm]	119.15	
Tumble ratio	1.34	
Valve timing	IVO	BTDC 35° CA
	IVC	ABDC 65° CA
	EVO	BDDC 20° CA
	EVC	ATDC 40° CA

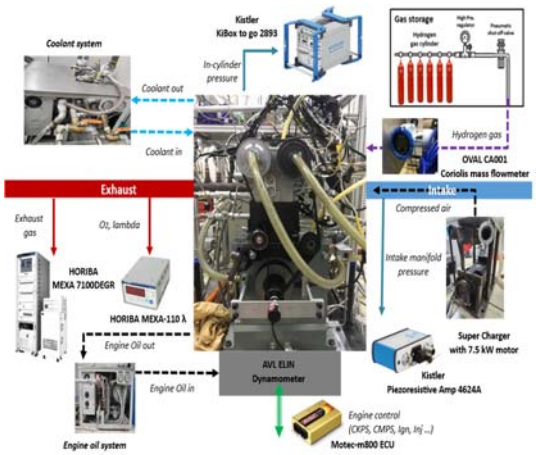

Figure 1: Schematic of the experimental setup

Table 2: Specifications for sensors and equipment.

Sensors/Equipment	Specifications	
Kistler 6056A	Linearity	< ±0.4%FSO
Kistler 4007C	Linearity	< ±0.2%FSO
`Kistler Kibox to go 2893	Uncertainty	<< 1 cycle
OVAL CA001	Uncertainty	< ±0.2%
Horiba MEXA-110 λ	Accuracy	0.9%
Horiba MEXA-7100 DEGR	Uncertainty	< 1.0%

2.2 Experimental Procedure

The engine speed was fixed at 1500 rpm for all the experimental cases. The throttle was fully opened, and the intake pressure varied from 0.10 MPa to 0.14 MPa with an interval of 0.02 MPa.

The fuel injection timing was set before top dead center (BTDC) at 80° CA. The ignition timing was set to the maximum brake torque (MBT) timing, which was after top dead center (ATDC) 7° CA.

The relative air-to-fuel ratio was controlled by varying the injected fuel quantity, ranging from the rich limit up to λ=3.5, 4.0, and 4.5 for intake pressures of 0.10, 0.12, and 0.14 MPa, respectively. The rich limit was defined as the condition at which the maximum pressure rise rate (MPRR) reached 0.5 MPa/°CA.

The leanest relative air-to-fuel ratio for each intake pressure was defined as the condition where λ exceeded the value corresponding to the maximum thermal efficiency by 0.5. The detailed experimental conditions are presented in **Table 3**.

2.3 Thermodynamic-based Combustion Analysis

To analyze the combustion results and characteristics, **Equations (1)-(5)** from Heywood **[6]** were used. All values were calculated from the average values over 200 cycles.

GMEP was calculated via **Equation (1)**.

$$GMEP = \frac{\int_{V_{BDC}}^{V_{TDC}} P_{compression} dV + \int_{V_{TDC}}^{V_{BDC}} P_{Expansion} dV}{V_d} \quad (1)$$

where V_{TDC} is the in-cylinder volume at the top dead center (TDC), V_{BDC} is the in-cylinder volume at the bottom dead center (BDC), $P_{compression}$ is the in-cylinder pressure during the compression stroke, $P_{Expansion}$ is the in-cylinder pressure during the expansion stroke, and V_d is the displaced volume.

Table 3: Experimental conditions

Parameters	Values		
Engine speed [rpm]	1500		
Throttle position	Wide open throttle		
Intake pressure [MPa]	0.10	0.12	0.14
Fuel injection pressure [MPa]	3		
Ignition timing	MBT timing (MFB50=ATDC 7° CA)		
Rich limit [MPa/°CA]	0.5		
Relative Air-to-fuel ratio [λ] at each intake pressure	0.10 MPa	From 1.98 to 3.5	
	0.12 MPa	From 2.20 to 4.0	
	0.14 MPa	From 2.45 to 4.5	

The gross thermal efficiency was calculated using **Equation (2)**.

$$GTE\ (\%) = \frac{\int_{V_{BDC}}^{V_{TDC}} P_{compression} dV + \int_{V_{TDC}}^{V_{BDC}} P_{Expansion} dV}{m_{fuel} \times Q_{LHV}} \times 100 \quad (2)$$

where m_{fuel} is the mass of fuel injected into the cylinder per cycle and Q_{LHV} is the lower heating value of the hydrogen.

The heat release rate (HRR) was calculated using **Equation (3)**.

$$HRR = \frac{\gamma}{\gamma-1} P \frac{dV}{d\theta} + \frac{1}{\gamma-1} V \frac{dP}{d\theta} \quad (3)$$

where the specific heat ratio, γ, is assumed to be 1.3 and where θ is the CA, P is the in-cylinder pressure, and V is the in-cylinder volume.

The HRR was summed cumulatively concerning the CA to obtain the cumulative HRR. The CA at which the cumulative HRR reached its maximum value, designated as the end of combustion, was used to calculate the mass fraction burned (MFB) percentile.

The MPRR was calculated by **Equation (4)**.

$$MPRR = \left(\frac{dP}{d\theta}\right)_{maximum} \quad (4)$$

The coefficient of variation of the GMEP (CoV_{GMEP}) was calculated by **Equation (5)**.

$$CoV_{GMEP}(\%) = \frac{\sigma_{GMEP}}{GMEP} \times 100 \quad (5)$$

where σ_{GMEP} is the standard deviation of the GMEP for 200 cycles.

3. Results and Discussions

3.1 Analysis of Combustion Characteristics

As shown in **Figure 2**, the peak in-cylinder pressure increased with increasing intake pressure. Specifically, the peak in-cylinder pressures for intake pressures of 0.10, 0.12, and 0.14 MPa were 4.77, 6.37, and 7.37 MPa, respectively. Because the intake of higher-density air through the supercharger enabled the injection of a greater amount of hydrogen under the same relative air-to-fuel ratio, a higher peak in-cylinder pressure was achieved.

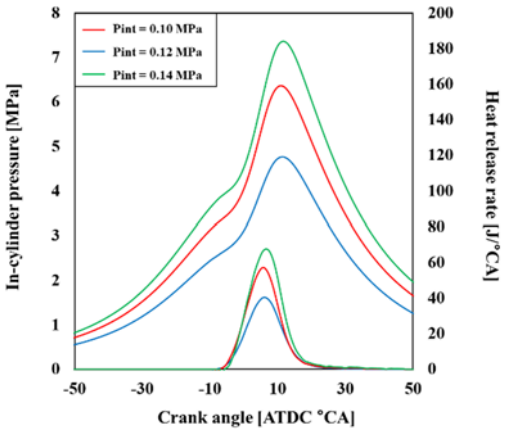

Figure 2: In-cylinder pressure and heat release rate for various intake pressures at λ=3.0.

Additionally, the peak HRR increased as the intake pressure increased. This phenomenon indicates that increasing the intake pressure promotes more efficient combustion of air/fuel mixtures, even under the same relative air-to-fuel ratio conditions. The faster burn duration with increasing intake pressure, as shown in **Figure 3**, indicates that a higher intake pressure facilitates more efficient combustion.

Additionally, the faster combustion with increasing intake pressure caused retardation of the ignition timing according to the increase in intake pressure to maintain the same MBT timing, as shown in **Figure 4**.

Specifically, at λ=3.0, the ignition timing for an intake pressure of 0.10 MPa was BTDC 9.0° CA, whereas the ignition timing values for intake pressures of 0.12 and 0.14 MPa were BTDC 8.2° and 6.8° CA, respectively. These tendencies were observed across various relative air-to-fuel ratios.

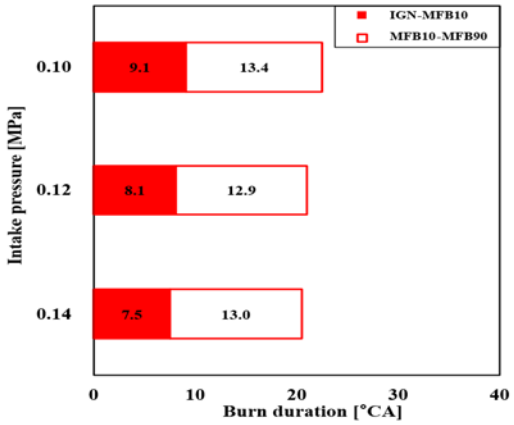

Figure 3: Burn duration for various intake pressures at λ=3.0

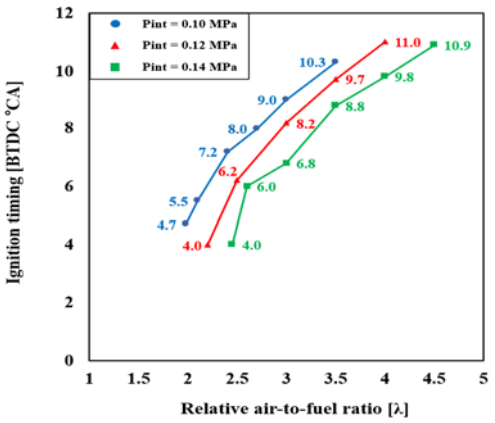

Figure 4: Ignition timing for various intake pressures under various relative air-to-fuel ratios.

A detailed analysis of burn duration provides further insights into the influence of intake pressure on combustion. For example, although the increase in intake pressure generally shortened the overall burn duration, the initial burn duration (IGN–MFB10 duration) was further shortened compared with the main combustion duration (MFB10–MFB90 duration). Specifically, when the intake pressure increased from 0.10 MPa to 0.14 MPa, the MFB10–MFB90 duration decreased by 0.4° CA, whereas the IGN–MFB10 duration decreased by 1.6° CA.

Because the IGN-MFB10 duration represents the flame development duration **[6]**, these experimental results indicate that increasing the intake pressure can facilitate fast flame development in H_2 DISI engines.

Additionally, considering that fast flame development causes more stable combustion under lean conditions **[6][14]**, the extension of the operable relative air-to-fuel ratio to leaner conditions with higher intake pressures can be attributed to the shorter IGN-MFB10 duration of the higher intake pressure.

As shown in **Figure 5**, at λ=3.0, the CoV_{GMEP} values for intake pressures of 0.10, 0.12, and 0.14 MPa were 2.70, 0.89, and 0.67%, respectively. Furthermore, CoV_{GMEP} for the intake pressure of 0.10 MPa was 5.79% at λ=3.5, whereas it decreased to 2.01% at 0.12 MPa and further decreased to 1.08% at 0.14 MPa and λ=4.5. Additionally, **Figure 6** shows that although the leanest relative air-to-fuel ratio became leaner with increasing intake pressure, the IGN–MFB10 duration was similar across all the intake pressures. These results indicate that increasing the intake pressure can improve the combustion stability in H_2 DISI engines under ultra-lean conditions.

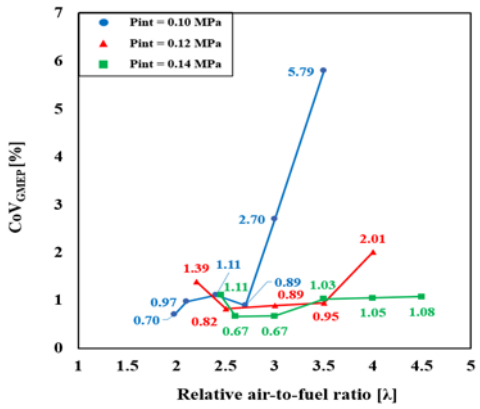

Figure 5: CoV_{GMEP} for various intake pressures under various relative air-to-fuel ratios

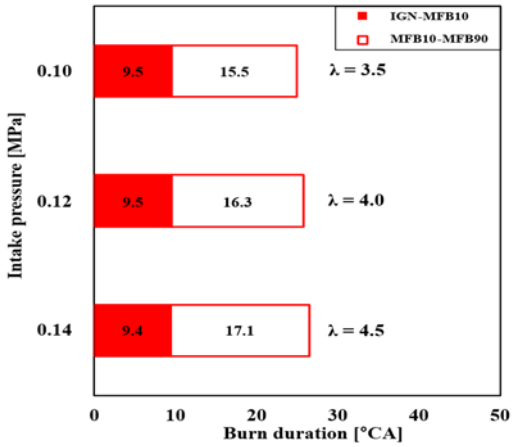

Figure 6: Burn duration under the leanest relative air-to-fuel ratios for each intake pressure

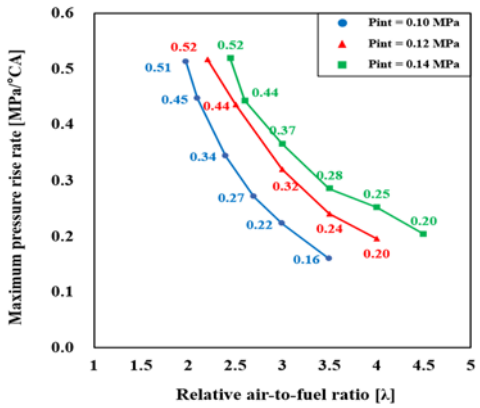

Figure 7: Maximum pressure rise rate for various intake pressures under various relative air-to-fuel ratios

On the other hand, the faster flame development with higher intake pressure limited the increase of the rich limit. Specifically, the rich limits for intake pressures of 0.10, 0.12, and 0.14 MPa were λ=1.98, 2.20, and 2.45, respectively.

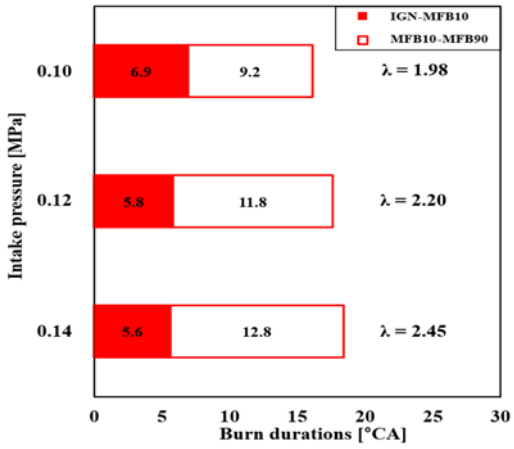

Figure 8: Burn duration at the rich limit for each intake pressure

Figure 7 indicates that the MPRR for each intake pressure at their rich limit exceeded the MPRR limit set at 0.5 MPa/°CA. This phenomenon can be attributed to the fact that with increasing intake pressure, the fast combustion at the IGN-MFB10 duration caused a rapid rise in pressure, resulting in the formation of the rich limit at a leaner relative air-to-fuel ratio **[9]**.

As illustrated in **Figure 8**, the IGN-MFB10 duration decreased with increasing intake pressure, even under a leaner relative air-to-fuel ratio.

3.2 Analysis of thermal Efficiency, Engine Performance, and NO_x Emissions

The gross thermal efficiency (GTE) increased with increasing intake pressure under various relative air-to-fuel ratios, as shown in **Figure 9**.

Specifically, the GTEs for intake pressures of 0.10, 0.12, and 0.14 MPa at λ=3.0 were 46.12, 46.55, and 46.75%, respectively.

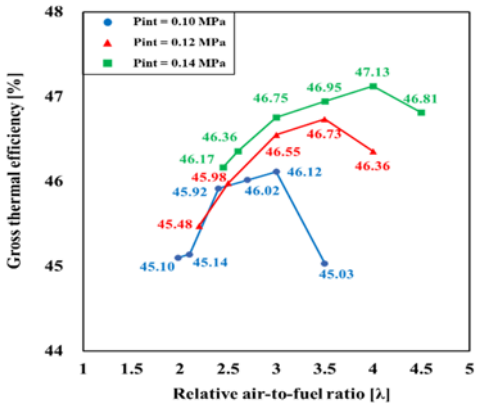

Figure 9: Gross thermal efficiency for various intake pressures under various relative air-to-fuel ratios.

The more efficient combustion of the higher intake pressure induced by the faster burn duration and higher in-cylinder flow, as explained in Section 3.1, is attributed to an increase in the GTE **[9]**.

A key observation is that the relative air-to-fuel ratio corresponding to the maximum GTE tends to be leaner with increasing intake pressure. Specifically, the maximum GTE for the intake pressure of 0.10 MPa was 46.12% at λ=3.0, whereas it was 46.73% at λ=3.5 and 47.13% at λ=4.0 for intake pressures of 0.12 and 0.14 MPa, respectively. These results can be attributed to the effect of lean combustion, resulting in increased thermal efficiency **[6][7][17]**.

As explained in Section 3.1, because combustion stability improved with increasing intake pressure, resulting in leaner operation, the maximum GTE was achieved at a leaner relative air-to-fuel ratio. These results indicate that increasing the intake pressure can increase the thermal efficiency in H_2 DISI engines by improving the combustion stability under ultra-lean conditions and extending the operable relative air-to-fuel ratio toward leaner conditions.

Additionally, increasing the intake pressure increased the GMEP under various relative air-to-fuel ratios, as shown in **Figure 10**.

Notably, although a rich limit for the higher intake pressure was formed at the leaner relative air-to-fuel ratio, as explained in Section 3.1, the maximum GMEP increased with increasing intake pressure. For example, when the intake pressure increased from 0.10 MPa to 0.14 MPa, the maximum GMEP increased from 0.80 MPa to 1.02 MPa, corresponding to an increase of approximately 20%.

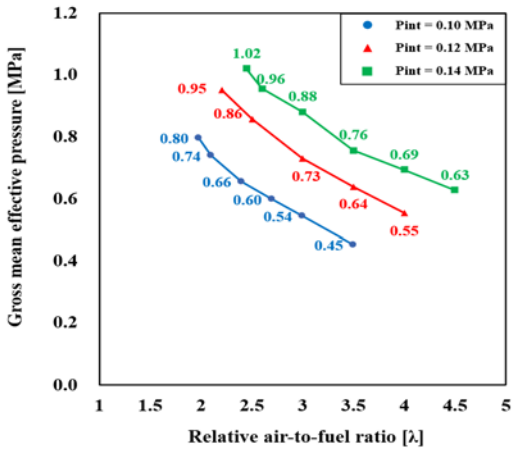

Figure 10: Gross mean effective pressure for various intake pressures under various relative air-to-fuel ratios.

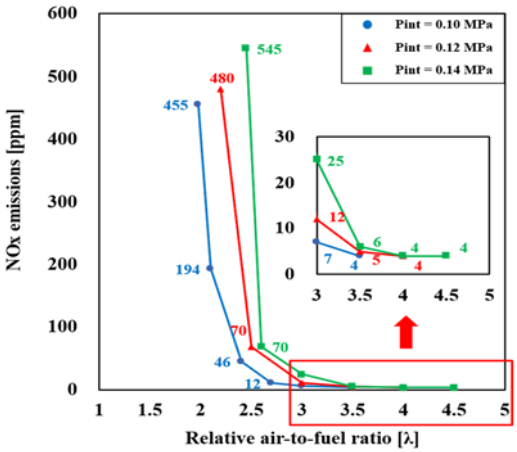

Figure 11: NOx emissions for various intake pressures under different relative air-to-fuel ratios

Additionally, even under the leanest condition for each intake pressure, the GMEP for an intake pressure of 0.14 MPa was 40% greater than that for an intake pressure of 0.10 MPa. These results show that increasing the intake pressure can be an effective method to increase engine loads in H_2 DISI engines.

Although increasing the intake pressure effectively increased the engine load, the NOx emissions also increased with increasing intake pressure, as shown in **Figure 11**.

NOx emissions for an intake pressure of 0.14 MPa were 545 ppm, whereas those for an intake pressure of 0.10 MPa were 455 ppm at rich limit conditions for each intake pressure. Although the relative air-to-fuel ratio was leaner for higher intake pressures, NOx emissions increased due to an increase in engine loads. For the same reason, even under the same relative air-to-fuel ratio of λ=3.0, the NOx emissions at an intake pressure of 0.14 MPa were more than 3 times higher than those at an intake pressure of 0.10 MPa. These results indicate that further research for suppressing the formation of NOx emissions resulting from an increase in engine loads is needed.

On the other hand, NOx emissions for each intake pressure were emitted similarly under relative air-to-fuel ratios greater than λ=3.5. For example, at λ=3.5, the NOx emissions at intake pressures of 0.10, 0.12, and 0.14 MPa were 4, 5, and 6 ppm, respectively. Furthermore, as the relative air-to-fuel ratios became leaner than λ=3.5 for intake pressures of 0.12 and 0.14 MPa, only 4 ppm of NOx emissions were emitted. These results can be attributed to the suppression of NOx emissions due to the low combustion temperature resulting from ultra-lean combustion **[17][18]**.

Meanwhile, in medium-to-low load conditions, operating the

engine under an intake pressure of 0.14 MPa at λ=4.0 resulted in the highest thermal efficiency and the lowest NOx emissions with high combustion stability as explained in Section 3.1.

4. Conclusion

This study analyzed the effects of increasing intake pressure by adopting a supercharger under various relative air-to-fuel ratios on the combustion characteristics, engine performance, and NOx emissions of a 0.5 L H_2 DISI engine.

Increasing the intake pressure resulted in more stable combustion under ultra-lean relative air-to-fuel ratios because of faster flame development. In other words, increasing the intake pressure extended the operable relative air-to-fuel ratio toward leaner conditions. Specifically, unlike an intake pressure of 0.10 MPa, which resulted in a CoV_{GMEP} of 5.79% at λ=3.5, the CoV_{GMEP} value for an intake pressure of 0.14 MPa was 1.08%, even at λ=4.5.

Changing the operable relative air-to-fuel ratio toward lean conditions resulted in a higher maximum GTE with the same amounts of NOx emissions as those for the intake pressure of 0.10 MPa due to leaner combustion. While the maximum GTE for the intake pressure of 0.10 MPa was 46.12%, with 4 ppm NOx emissions at λ=3.0, it increased to 47.13% at 0.14 MPa with the same NOx level at λ = 4.0. Notably, under this operating condition, the highest GTE and the lowest NOx emissions were achieved with high combustion stability with the CoV_{GMEP} of 1.05% and a corresponding GMEP of 0.69 MPa.

Additionally, increasing the intake pressure increased the engine load. Although the faster flame development with higher intake pressures limited further increases in the rich limit, the maximum GMEP increased as the intake pressure increased. Specifically, the maximum GMEP for an intake pressure of 0.14 MPa was 1.02 MPa at λ=2.45, whereas it was 0.80 MPa at λ=1.98 for an intake pressure of 0.10 MPa.

The major concern with increasing intake pressure was the rapid increase in NOx emissions greater than λ=3.0. For example, NOx emission increased from 455 ppm to 545 ppm as the intake pressure increased from 0.10 MPa to 0.14 MPa. These results indicate the necessity of further research on methods for suppressing the formation of NOx emissions including retarding ignition timing, implementing a water injection system or adopting an exhaust gas after-treatment system under high-load conditions in an H_2 DISI engine **[9][19]-[21]**.

Acknowledgement

This research paper was written with the support of the 2025 Academic Research Project of the Naval Institute for Ocean Research of the Republic of Korea Naval Academy. The experimental research for writing this paper was carried out at the Automotive Laboratory of Seoul National University, which participated in the research and development project of the Ministry of Trade, Industry and Energy (NO. 20018473) and the National Research Foundation (No. 2021R1G1A1004451).

Author Contributions

Conceptualization, K. D. Min; Methodology, S. J. Kim and H. M. Lee; Software, S. J. Kim; Formal Analysis, S. J Kim and H. M. Lee; Investigation, S. J. Kim; Resources, K. D. Min; Data Curation S. J. Kim; Writing-Original Draft Preparation, S. J. Kim and H. M. Lee; Writing-Review & Editing, H. M. Lee; Visualization, S. J. Kim and H. M. Lee; Supervision, K. D. Min; Project Administration, S. J. Kim and H. M. Lee; Funding Acquisition, H. M. Lee and K. D. Min.

References

[1] IEA, https://www.iea.org/data-and-statistics/charts/global-co2-emissions-from-transport-by-sub-sector-in-the-net-zero-scenario-2000-2030-2, Accessed April 27, 2025

[2] IEA, https://www.iea.org/reports/credible-pathways-to-150c, Accessed April 27, 2025

[3] J. Kim, C. Huh, and Y. Seo, “End-to-end value chain analysis of isolated renewable energy using hydrogen and ammonia energy carrier,” Energy Conversion and Management, vol. 254, 115247, 2022. Available: https://doi.org/10.1016/j.enconman.2022.115247.

[4] S. Verhelst and T. Wallner, “Hydrogen-fueled internal combustion engines,” Progress in Energy and Combustion Science, vol. 35, no. 6, pp. 490-527, 2009. Available: https://doi.org/10.1016/j.pecs.2009.08.001.

[5] D. C. North, “An investigation of hydrogen as an internal combustion fuel,” International Journal of Hydrogen Energy, vol. 17, no. 7, pp. 509-512, 1992. Available: https://doi.org/10.1016/0360-3199(92)90150-U.

[6] J. Heywood, Internal Combustion Engine Fundamentals, New York: McGraw-Hill, 1988.

[7] T. Wallner, H. Lohse-Busch, and N. Shidore, “Operating strategy for a hydrogen engine for improved drive-cycle

efficiency and emissions behavior," International Journal of Hydrogen Energy, vol. 34, no. 10, pp. 4617-4625, 2009. Available: https://doi.org/10.1016/j.ijhydene.2008.07.099.

[8] Z. Fu, Y. Li, W. Wu, Y. Li, and W. Gao, "Experimental study on the combustion and emission performance of the hydrogen direct injection engine," International Journal of Hydrogen Energy, vol. 61, pp. 1047-1059, 2024. Available: https://doi.org/10.1016/j.ijhydene.2024.02.276.

[9] S. Lee, Optimization of Combustion Chamber and Load Expansion in a Hydrogen Direct Injected Spark Ignition Engine, Ph. D. Dissertation, Department of Mechanical Engineering, Seoul National University, Republic of Korea, 2024.

[10] S. Verhelst, P. Maesschalck, N. Rombaut, and R. Sierens, "Increasing the power output of hydrogen internal combustion engines by means of supercharging and exhaust gas recirculation," International Journal of Hydrogen Energy, vol. 34, no. 10, pp. 4406-4412, 2009. Available: https://doi.org/10.1016/j.ijhydene.2009.03.037.

[11] D. Nguyen, Y. Choi, C. Park, Y. Kim, and J. Lee, "Effect of supercharger system on power enhancement of hydrogen-fueled spark-ignition engine under low-load condition," International Journal of Hydrogen Energy, vol. 46, no. 9, pp. 6928-6936, 2021. Available: https://doi.org/10.1016/j.ijhydene.2020.11.144.

[12] Z. Stępień, "A comprehensive overview of hydrogen-fueled internal combustion engines: Achievements and future challenges," Energies, vol. 14, no. 20, 6504, 2021. Available: https://doi.org/10.3390/en14206504.

[13] C. M. White, R. R. Steeper, and A. E. Lutz, "The hydrogen-fueled internal combustion engine: a technical review," International Journal of Hydrogen Energy, vol. 31, no. 10, pp. 1292-1305, 2006.

[14] S. Kim, Optimization of a Split Injection Strategy in a Hydrogen Direct-Injection Spark Ignition Engine, Master's Thesis, Department of Mechanical Engineering, Seoul National University, Republic of Korea, 2025.

[15] Z. Liang, F. Xie, K. Lai, H. Chen, J. Du, and X. Li, "Study of single and split injection strategies on combustion and emissions of hydrogen DISI engine," International Journal of Hydrogen Energy, vol. 49, pp. 1087-1099, 2024.

[16] Z. Hu, S. Yuan, H. Wei, Z. Huang, H. Wei, S.H. Chan, and L. Zhou, "High-pressure injection or low-pressure injection for a direct injection hydrogen engine?," International Journal of Hydrogen Energy, vol. 59, pp. 383-389, 2024.

[17] T. D. Fansler, D. L. Reuss, V. Sick, and R. N. Dahms, "Invited Review: Combustion instability in spray-guided stratified-charge engines: A review," International Journal of Engine Research, vol. 16, no. 3, pp. 260-305, Apr. 2015, Available: https://doi.org/10.1177/1468087414565675.

[18] V. Kumar, D. Gupta, and N. Kumar, "Hydrogen use in internal combustion engine: A review," International Journal of Advanced Culture Technology, vol. 3, no. 2, pp. 87-99, 2015. Available: https://doi.org/10.17703/IJACT.2015.3.2.87.

[19] V. Subramanian, J.M. Mallikarjuna, A. Ramesh, "Effect of water injection and spark timing on the nitric oxide emission and combustion parameters of a hydrogen fuelled spark ignition engine," International Journal of Hydrogen Energy, vol. 21, no. 9, pp. 1159-1173, 2007. Available: https://doi.org/10.1016/j.ijhydene.2006.07.022.

[20] P. Xu, C. Ji, S. Wang, X. Cong, Z. Ma, C. Tang, H. Meng, and C. Shi, "Effects of direct water injection on engine performance in a hydrogen (H_2)-fueled engine at varied amounts of injected water and water injection timing," International Journal of Hydrogen Energy, vol. 45, no. 24, pp. 13523-13534, 2020. Available: https://doi.org/10.1016/j.ijhydene.2020.03.011.

[21] S. Sterlepper, M. Fischer, J. Claßen, V. Huth, and S. Pischinger, "Concepts for hydrogen internal combustion engines and their implications on the exhaust gas aftertreatment system," Energies, vol. 14, no. 23, 8166, 2021. Available: https://doi.org/10.3390/en14238166.